Journal of Materials Chemistry A

PAPER

View Article Online
View Journal | View Issue

Cite this: J. Mater. Chem. A, 2015, 3, 7773

Single-ion dominantly conducting polyborates towards high performance electrolytes in lithium batteries†

Bingsheng Qin,[ab] Zhihong Liu,*[b] Jie Zheng,[b] Pu Hu,[b] Guoliang Ding,[b] Chuanjian Zhang,[b] Jianghui Zhao,[b] Desheng Kong*[a] and Guanglei Cui*[b]

Received 10th January 2015
Accepted 4th March 2015

DOI: 10.1039/c5ta00216h

www.rsc.org/MaterialsA

A couple of thermally stable polyborate salts, polymeric lithium pentaerythrite borate (PLPB) and polymeric lithium di(trimethylolpropane)borate (PLDB), for applications in lithium ion batteries were synthesized *via* a facile one-step reaction in aqueous solution. Both the lithium polyborate salts exhibited a high thermal decomposition temperature at about 240 °C. Besides, their corresponding single-ion dominantly conducting gel polymer electrolytes of ethylene carbonate (EC) and dimethyl carbonate (DMC) (1 : 1, v/v) swollen PLPB@PVDF-HFP (poly(vinylidenefluoride-*co*-hexafluoropropene)) and PLDB@PVDF-HFP exhibited favorable ionic conductivity over a wide temperature range, superior electrochemical stability, high lithium ion transference number and Al passivating ability. The Li/$LiFePO_4$ batteries using these single-ion dominantly conducting electrolytes exhibited stable charge–discharge behavior and excellent cycling performance both at room temperature and at elevated temperatures. These superior performances could make this class of gel polymer electrolytes very promising candidates for lithium batteries especially at elevated temperatures.

1. Introduction

Lithium batteries have attracted extensive interest owing to their recent application in large scale energy storage systems such as hybrid electric vehicles (HEVs), electric vehicles (EVs) and smart grids.[1,2] To achieve large scale applications, lithium batteries with low cost, high performance and better safety characteristics are highly desirable.[3–5] $LiPF_6$ is the predominant lithium salt used in state-of-the-art lithium ion batteries. The $LiPF_6$ based electrolyte possesses overall performance such as superior ionic conductivity, satisfactory electrochemical window, favorable interface forming properties on graphite anodes and passivation on an Al current collector when compared to other lithium salts. Therefore, the $LiPF_6$ based electrolyte is considered to be quite successful in batteries for use in consumable electronic devices.[6,7] However, $LiPF_6$ is known to degrade in organic carbonate solvents, which will be accelerated at elevated temperatures or catalyzed by traces of water in the electrolyte. The decomposition products consist of HF and PF_5, where HF can dissolve metal moieties in cathode materials and PF_5 can react with carbonate solvents, thus reducing the battery capacity and increasing the impedance of the battery. In addition, the $LiPF_6$ based liquid electrolyte using a large amount of flammable organic solvents also raises the safety problem.[8–12] Besides, in terms of large scale applications such as in HEVs, EVs and smart grids, the $LiPF_6$ based liquid electrolyte has severe limitations owing to its expensiveness and intricate processing. Therefore, it is imperative to develop new lithium salts with superior thermal and electrochemical stabilities, cost effectiveness and environmental benignity.

In the past several decades, numerous efforts have been dedicated to striving for major breakthroughs in the core technology of novel lithium salts.[13–15] Among them, lithium borate salts such as lithium bis(oxalato)borate (LiBOB)[16–20] and lithium oxalyldifluoroborate (LiODFB)[21–25] have drawn intensive attention owing to their unique properties of excellent thermal stability, comparable ionic conductivity, cost-effectiveness, environmental benignity and favorable solid electrolyte interface forming properties. Very recently, several single-ion conducting polymeric lithium borate salts, including lithium polyvinyl alcohol oxalate borate (LiPVAOB),[26] lithium polyacrylic acid oxalate borate (LiPAAOB),[27] lithium polymeric tartaric acid

[a]Shandong Province Key Laboratory of Life-Organic Analysis, School of Chemistry and Chemical Engineering, Qufu Normal University, Qufu, 273165, China. E-mail: kongdscn@eyou.com

[b]Qingdao Key Laboratory of Solar Energy & Energy Storage, Qingdao Institute of Bioenergy and Bioprocess Technology, Chinese Academy of Sciences, Qingdao 266101, China. E-mail: liuzh@qibebt.ac.cn; cuigl@qibebt.ac.cn

† Electronic supplementary information (ESI) available: ^1H NMR spectra of pentaerythrite, di(trimethylolpropane), PLPB and PLDB in DMSO-d_6, XRD patterns and typical SEM images of PLPB and PLDB, the molecular mass per unit of the polymeric lithium salts synthesized in recent years, stress–strain curves for PLPB@PVDF-HFP and PLDB@PVDF-HFP membranes, AC impedance of Li/GPEs/Li cells before and after being polarized with a potential difference of 10 mV at room temperature, and cycling performance and charge–discharge profiles of the Li/PC swollen PLPB@PVDF-HFP/$LiFePO_4$ batteries at 120 °C. See DOI: 10.1039/c5ta00216h

borate (PLTB)[28,29] and some lithium aromatic polyborates (*e.g.* LiPPAB),[30,31] were developed and some of them were demonstrated to be very promising in lithium ion batteries. For example, LiPAAOB and LiPVAOB based composite membranes were demonstrated to be very promising for LIB gel polymer electrolytes.[32,33] In addition, the batteries using EC/DMC-PLTB@PVDF-HFP electrolytes prepared in our laboratory exhibited significantly improved cycle performance at an elevated temperature of 55 °C, which outperformed the batteries using conventional $LiPF_6$-based electrolytes.[34]

Herein, based on the above design concepts, a couple of polyborate salts named PLPB and PLDB were synthesized from lithium hydroxide, boric acid and pentaerythrite and di(trimethylolpropane) respectively *via* a facile one-step reaction in aqueous solution. Both the lithium salts exhibited a high thermal decomposition temperature at about 240 °C. Their corresponding gel polymer electrolytes, *i.e.*, EC/DMC swollen PLPB@PVDF-HFP and PLDB@PVDF-HFP, will be discussed in detail in terms of electrochemical stability, ionic conductivity, lithium ion transference number and Al passivating ability. The Li/$LiFePO_4$ batteries using the EC/DMC swollen PLPB@PVDF-HFP single-ion conducting electrolyte were also systematically evaluated regarding the charge–discharge behavior and cycling performance both at room temperature and at elevated temperatures. The fascinating performance will make this single ion gel polymer electrolyte a promising candidate for next generation lithium batteries.

2. Experimental

2.1. Materials

Boric acid (99.99%, Alfa Aesar), lithium hydroxide monohydrate (GR, Aladdin), pentaerythrite (98%, J&K), di(trimethylolpropane) (97%, Aldrich), poly(vinylidenefluoride-*co*-hexafluoropropene) (PVDF-HFP, Aldrich, $M_w \sim 400\,000$), dimethyl sulfoxide (DMSO, 99.5%, Sinopharm Chemical Reagent Co., Ltd), cyclohexane (AR, Fu Yu Co., Ltd), $LiPF_6$ (99.99%, Aldrich), ethylene carbonate (EC), propylene carbonate (PC) and dimethyl carbonate (DMC) (all from Capchem Technology Co., Ltd), and $LiFePO_4$ (Tianjin Strain Energy Science and Technology Ltd, particle size: 3 ± 1.0 μm, carbon content: 1.5–2.0 wt%) were used. All the reagents were used without further purification.

2.2. Synthesis and characterization of PLPB and PLDB

The procedure for the synthesis of PLPB and PLDB is shown in Scheme 1. Firstly, 0.03 mol pentaerythrite (4.0845 g) and 200 mL deionized water were added into a 500 mL three-necked flask equipped with a Dean–Stark adaptor and stirred for 1 h at 60 °C to obtain a homogeneous solution. After that, equimolar amounts of boric acid (0.03 mol, 1.8549 g) and lithium hydroxide monohydrate (0.03 mol, 1.2589 g) were dissolved and mixed in 100 mL deionized water and then added dropwise to the above homogeneous solution and allowed to react for 2 hours at 100 °C. Then 100 mL cyclohexane was added into the flask for azeotropic water removal to precipitate the white product. All the synthetic processes were performed under an argon atmosphere. After the water was completely removed, the white precipitate was filtered, collected and dried at 120 °C under vacuum to afford 4.5 g PLPB. The synthesis process of PLDB was similar to that of PLPB and 8.1 g PLDB was obtained.

^1H NMR spectra of the products dissolved in DMSO-d_6 were recorded on a nuclear magnetic resonance spectrometer (Bruker Avance-III). The thermal behavior of PLPB and PLDB was evaluated on a thermogravimetric analyzer (TGA, Rubotherm-Dyntherm-HP) under an Ar atmosphere at a heating rate of 10 °C min^{-1}. X-ray diffraction (XRD) measurements were carried out to characterize the phase purity and crystalline structure of the prepared polymeric lithium borates using a Bruker-AXS micro-diffractometer (D8 ADVANCE) with Cu-K radiation ($\lambda = 1.5406$ Å) from 5° to 80° at a scanning speed of 0.33° min^{-1}. The surface morphology of both polymeric lithium salts was observed with a Hitachi S-4800 field emission scanning electron microscope (FE-SEM).

2.3. Preparation and characterization of the single-ion dominantly conducting GPEs

0.5 g PLPB and 0.5 g PVDF-HFP were added into 8 mL anhydrous DMSO and stirred to obtain a homogeneous solution. Then the PLPB@PVDF-HFP membrane was prepared by a doctor-blading process followed by vacuum drying at 80 °C for 24 hours to remove the DMSO solvent. The mechanical strength of the membranes was characterized by stress–strain curves which were evaluated using an Inston-3300 universal testing machine with a stretching speed of 1.66 mm s^{-1}. The surface morphology of both polymer membranes was observed by FE-SEM and the distribution of the B element was evaluated by energy dispersive X-ray spectroscopy mapping (EDX, HoRiBA 7593-H). Then the as-prepared membrane was swollen by EC/DMC mixed solvents. The weight ratio of the solvents and dry membrane was about 2 : 1. The thickness of EC/DMC swollen PLPB@PVDF-HFP membranes was about 70 μm. The procedure for the preparation of EC/DMC swollen PLDB@PVDF-HFP was the same as that used for EC/DMC swollen PLPB@PVDF-HFP while the thickness of the membrane was about 80 μm.

2.4. Electrochemical characterization of single-ion dominantly conducting GPEs

The electrochemical stability of EC/DMC swollen PLPB@PVDF-HFP and PLDB@PVDF-HFP membranes as well as the commercially available EC/DMC-$LiPF_6$ (1 mol L^{-1}) liquid electrolyte was evaluated by the linear sweep voltammetry

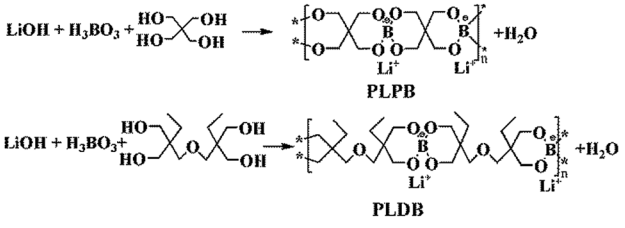

Scheme 1 Procedure for one-step synthesis of PLPB and PLDB in aqueous solution.

method performed on a stainless-steel working electrode and a lithium metal foil counter electrode at a scanning rate of 0.5 mV s^{-1}. The ionic conductivity of the dry membranes and single-ion dominantly conducting GPEs was measured between two stainless-steel plate electrodes and calculated by the formula as follows.

$$\sigma = \frac{L}{SR}$$

where L stands for the thickness of the GPE membranes and S stands for the area of the stainless steel electrode, and R is the resistance of the membranes, which can be obtained by the AC impedance analysis using a Zahner Zennium electrochemical workstation over a frequency range of 0.1–10^6 Hz. The lithium ion transference number (t_+) was measured by the method described by Evans *et al.*[35] The method involved sandwiching the sample membrane between two lithium electrodes. A DC potential of 10 mV was applied until a steady state was reached. The formula used to calculate the lithium ion transference number is as follows.

$$t_+ = \frac{I_s(\Delta V - I_0 R_0)}{I_0(\Delta V - I_s R_s)}$$

where t_+ is the cationic transference number, ΔV is the potential applied across the cell, R_0 and R_S are the initial and steady-state resistances of the passivating layers on the Li electrode, and I_0 and I_S are the initial and steady-state currents. The Al passivation measurement was evaluated by controlled potential coulometry performed on an Al foil working electrode and a lithium foil counter electrode. The measurements of electrochemical stability, lithium ion transference number and Al passivation ability were all conducted through a CHI660C Electrochemical Workstation (Shanghai, China).

2.5. Battery assembly and battery performance

A half coin cell (2032-type) was assembled by sandwiching the EC/DMC swollen PLPB@PVDF-HFP membrane between a lithium metal foil and the $LiFePO_4$ electrode. The $LiFePO_4$ electrode was composed of 80 wt% $LiFePO_4$ (around 3.0 mg active material on 1.54 cm^2 aluminum metal foil), 10 wt% PVDF and 10 wt% carbon black. All assembly of cells was carried out in an argon-filled glove box. The charge–discharge C-rate capacity and cycling ability of cells were recorded on a LAND battery test system. The galvanostatic charge–discharge behavior of Li/GPEs/$LiFePO_4$ cells was conducted over the range of 2.5–4.0 V.

3. Results and discussion

3.1. Characterization of PLPB and PLDB

The chemical structures of PLPB and PLDB were characterized by using the ^{1}H NMR measurement, which are shown in Fig. S1.† It was observed that the proton signals of –OH (4.19 ppm) for pentaerythrite disappeared after the reaction, and the proton signal of $-CH_2$ shifted downfield from 3.36 ppm to 3.52 ppm owing to the higher electron withdrawing property of the central B atom. These results suggested that the coordination polymerization between lithium hydroxide monohydrate, boron acid and pentaerythrite took place to form polymeric lithium borate. In the case of PLDB, the proton signal of –OH (4.19 ppm) for PLDB significantly decreased compared with that of di(trimethylolpropane) before the reaction, demonstrating the occurrence of the polymerization reaction between lithium hydroxide monohydrate, boron acid and di(trimethylolpropane). The proton signal of –OH did not completely disappear, indicating incomplete polymerization, which could be ascribed to a large steric hindrance in the case of di(trimethylolpropane). It is worth noting that PLPB possessed the highest lithium ion concentration per repeating unit (see Table S1†) among the novel polymeric lithium borate salts reported in recent years.

The FE-SEM images and XRD patterns of PLPB and PLDB particles are shown in Fig. S2.† Herein, PLPB displayed a spindrift-like morphology with a radius of approximately 0.5 μm, while PLDB displayed a rectangular shape with a size range of about 0.5 μm × 0.3 μm. The XRD patterns of PLPB and PLDB showed some sharp diffraction peaks between 5° and 30°, suggesting that the polymeric lithium salts possessed a typical semi-crystalline structure.[27]

The thermo-gravimetric analysis (TGA) curves of PLPB, PLDB and $LiPF_6$ are shown in Fig. 1. It could be seen that the commercially available lithium salt $LiPF_6$ started to decompose slowly at 70 °C and degrade rapidly at about 170 °C, which agreed well with the report in the literature.[32] In sharp comparison, both the polymeric lithium borate salts, PLPB and PLDB, exhibited a higher thermal decomposition temperature at about 240 °C, which could be attributed to their stable polyanionic structures. The superior thermal stability could make this kind of polymeric lithium borate very promising candidates for applications in LIBs operating at high temperatures. Besides, compared with PLTB (330 °C)[29] and LiBOB (302 °C),[18] the thermal decomposition temperature of PLPB and PLDB was relatively low, which is similar to that of LiODFB (240 °C). This could be a very critical feature for safety protection under extreme conditions such as mechanical circuit shorting and overcharge where the decomposition of PLPB and PLDB could serve as the safety vent for huge thermal runaway.[21]

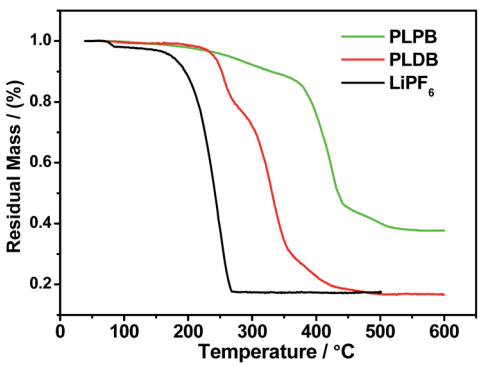

Fig. 1 Thermal gravimetric analysis curves of PLPB and PLDB under an argon atmosphere at a heating rate of 10 °C min^{-1}.

The stress–strain curves of PLPB@PVDF-HFP and PLDB@PVDF-HFP membranes are depicted in Fig. S3.† It was demonstrated that the PLPB@PVDF-HFP and PLDB@PVDF-HFP membranes possessed a tensile strength of 20 MPa with 5% strain and 14 MPa with 8% strain, respectively, which shows that they have potential for practical applications as polymer electrolytes. The surface morphologies of the PLPB@PVDF-HFP and PLDB@PVDF-HFP dry membranes are presented in Fig. 2. It was shown that both the membranes possessed a relatively smooth surface and no porous structure could be observed on the surface. The EDX mapping of the B element for both membranes is shown in Fig. 2(c) and (f), respectively. In both cases, the B element was homogeneously distributed on the membranes, indicating the uniformity of both membranes and good compatibility of these lithium borates with PVDF-HFP.

3.2. Electrochemical stability of the single ion dominantly conducting GPEs

The electrochemical stability of the EC/DMC swollen PLPB@PVDF-HFP and PLDB@PVDF-HFP membranes was evaluated by the linear sweep voltammetry (LSV) method and the commercially available EC/DMC-$LiPF_6$ electrolyte (1 mol L^{-1}) was taken as the control sample. The anodic current onset in the current–voltage curve was associated with the electrochemically oxidized decomposition of the electrolyte. As depicted in Fig. 3, the $LiPF_6$ based electrolyte started to oxidatively decompose at about 4.3 V at room temperature. By contrast, our EC/DMC swollen PLPB@PVDF-HFP and PLDB@PVDF-HFP membranes started to oxidatively decompose up to 4.6 V and 5.0 V, respectively, which was slightly higher than that of the LiBOB based electrolyte (4.5 V) as reported,[20] indicating their better electrochemical stability which might originate from the highly stable structure of the polyanions. The electrochemical stability determined by linear sweep voltammetry greatly depends on both thermodynamic and kinetic factors. PLDB itself was less structurally and thermodynamically stable than PLPB, because PLDB possessed ether links and more residual OH groups. However, the PLDB@PVDF-HFP electrolyte possessed a higher Li^+ transference number than that of PLPB@PVDF-HFP. That is to say, less anion moieties could move to the electrode surface and participate in the oxidative decomposition. Therefore, the whole PLDB@PVDF-HFP electrolyte was kinetically more stable than that of the PLPB@PVDF-HFP electrolyte. It is noteworthy that our result reflects the synergetic electrochemical stability of the electrolyte (solvent, PVDF-HFP and salt) not merely salt. In particular, the high electrochemical stability of EC/DMC swollen PLDB@PVDF-HFP up to 5.0 V could make it very promising for 5 V-class LIBs using cathode materials such as $LiNi_{0.5}Mn_{1.5}O_4$ and $LiCoPO_4$.

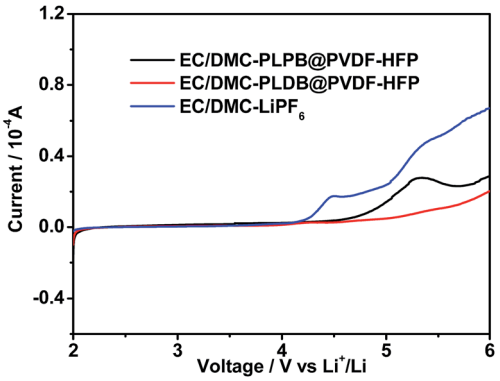

Fig. 3 Linear sweep voltammogram of EC/DMC-$LiPF_6$, EC/DMC swollen PLPB@PVDF-HFP and PLDB@PVDF-HFP electrolytes (scan rate = 0.5 mV s^{-1}).

3.3. Ionic conductivity and Li^+ transference number of the single ion dominantly conducting GPEs

Fig. 4 shows the temperature dependence of the ionic conductivity of EC/DMC swollen PLPB@PVDF-HFP and PLDB@PVDF-HFP electrolytes. The ionic conductivity of EC/DMC swollen PLPB@PVDF-HFP and PLDB@PVDF-HFP was about 1.8×10^{-4} S cm^{-1} and 1.2×10^{-4} S cm^{-1} at 30 °C, respectively, which were several orders of magnitude higher than those of the dry membranes and were valuable for practical applications. As the ion transport in single ion lithium borates is mainly achieved by lithium ions, the ionic conductivity of EC/DMC-PLPB@PVDF-HFP was a bit higher owing to the higher lithium ion concentration per repeating unit. It was shown that the ionic conductivity *vs.* temperature relationship agreed quite well with the Arrhenius equation over the temperature range between 30 °C and 80 °C. The activation energy (E_a) was 13.2 kJ mol^{-1} and 14.1 kJ mol^{-1} for EC/DMC swollen PLPB@PVDF-HFP and PLDB@PVDF-HFP electrolytes, respectively, which was comparable to that of other gel polymer electrolytes in the literature.[36,37]

The transference number of Li^+ for both single ion GPEs was further investigated and measured using the potential polarization method. Based on the resistance changes of the passivating layers (Fig. S4†) and current variation depicted in Fig. 5, an ultrahigh transference number t_+ of 0.84 and 0.89 was obtained for EC/DMC swollen PLPB@PVDF-HFP and PLDB@PVDF-HFP electrolytes, respectively, which is much higher than that of the conventional $LiPF_6$ based electrolyte[38,39]

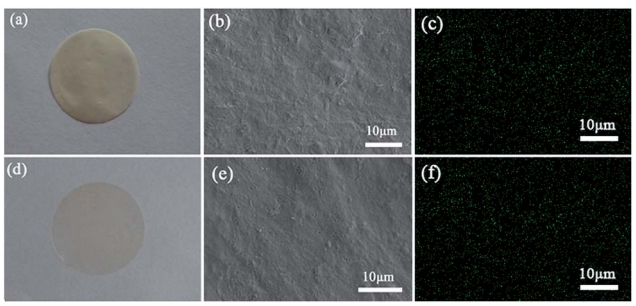

Fig. 2 The photograph (a), SEM image (b) and the EDX mapping of the B element (c) for the PLPB@PVDF-HFP membrane and the photograph (d), SEM image (e) and the EDX mapping of the B element (f) for the PLDB@PVDF-HFP membrane.

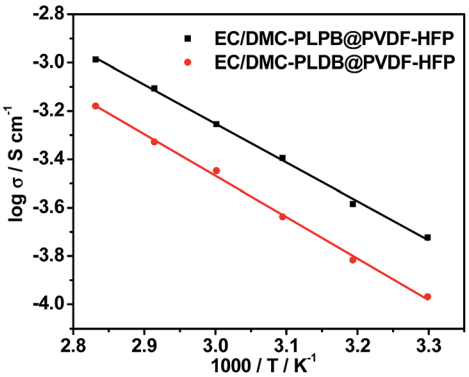

Fig. 4 Temperature dependence of the ionic conductivity of EC/DMC swollen PLPB@PVDF-HFP and PLDB@PVDF-HFP electrolytes.

and the LiBOB based electrolyte.[40] The Li^+ transference number of EC/DMC-PLDB@PVDF-HFP was slightly higher, which could be owing to a more complicated structure as well as higher steric hindrance of the PLDB polyanion. Besides, it was indicated that the ionic conductivity in the two GPEs was mainly contributed by Li^+ motion which will be of significant importance to reduce the polarization during the battery charging–discharging process as the electrode reactions only exchange the lithium ion in LIBs.

3.4. Al passivation of the single ion dominantly conducting GPEs

Al foil is commercially used in LIBs as a cathode current collector and its stability at high potentials in electrolytes depends on the effectiveness of the passivation film formed on the Al surface. Therefore, an important qualification that a new electrolyte system has to meet for its application in LIB technology is its ability to passivate Al at high potentials. As depicted in Fig. 6, the initial rapid decrease of the anodic current on a fresh Al surface suggested an instant formation of the passivation film. Subsequently, there were no signs of current increase with elapsed time at all potentials (from 4.00 V to 5.75 V *vs.* Li/Li^+), demonstrating that this passivated film displayed excellent stability for both GPEs even when the potential was stepped up to 5.75 V *vs.* Li/Li^+. Therefore, a preliminary conclusion from these results was made that both the single ion dominantly conducting GPEs were capable of effectively passivating and protecting the Al current collector.

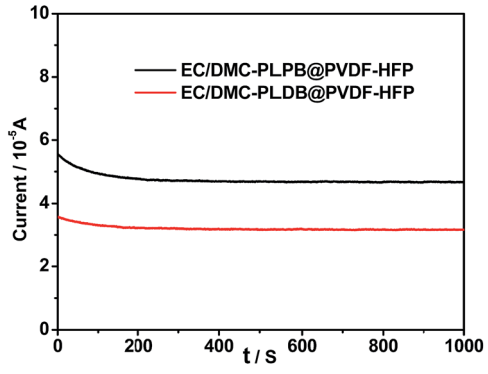

Fig. 5 Variation of current with time during polarization of the Li//EC/DMC swollen PLPB@PVDF-HFP membrane//Li cell and the Li//EC/DMC swollen PLDB@PVDF-HFP membrane//Li cell, with a total applied potential difference of 10 mV.

3.5. Battery performance of the single ion dominantly conducting GPEs

Owing to the higher ionic conductivity of EC/DMC swollen PLPB@PVDF-HFP, it was selected to evaluate the battery performance regarding the charge–discharge behaviors and cycle performance both at room temperature and at elevated temperatures. As can be seen from Fig. 7(a), the $Li/LiFePO_4$ battery using EC/DMC swollen PLPB@PVDF-HFP displayed a specific discharge capacity of 149 mA h g^{-1}, 138 mA h g^{-1} and 107 mA h g^{-1} at 0.1 C, 0.2 C and 0.5 C at room temperature, which increased to 161 mA h g^{-1}, 150 mA h g^{-1} and 122 mA h g^{-1}, respectively, at an elevated temperature of 60 °C. The improved rate capability should be unambiguously ascribed to the enhanced ionic conductivity of the GPE at elevated temperatures. Besides, the stable charge–discharge profiles at 0.1 C, 0.2 C and 0.5 C at 60 °C, as shown in Fig. 7(b), were quite typical for $Li/LiFePO_4$ batteries with a charge and discharge plateau around 3.4 V,[41] demonstrating the good compatibility between the polymeric lithium borate salt and the electrodes as well as the superior thermal and electrochemical stability of the as-prepared gel polymer electrolyte. Moreover, the excellent cycling performance and high coulombic efficiency of about 99.5% both at room temperature and at elevated temperatures

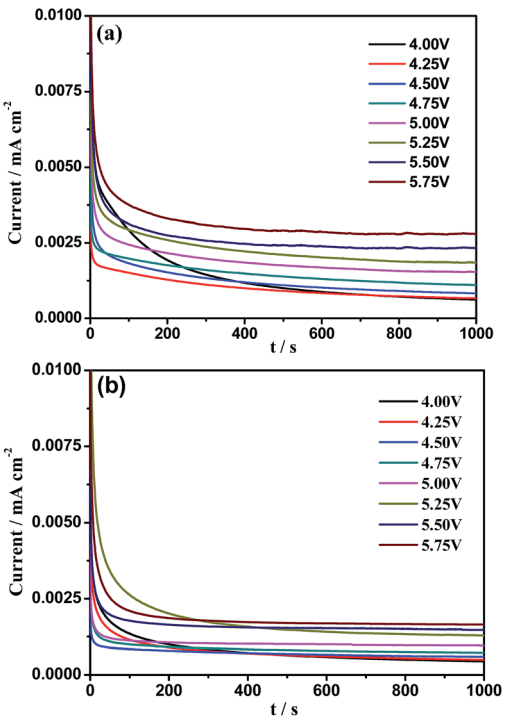

Fig. 6 Time-decaying current density obtained on an Al electrode at various potentials *vs.* Li^+/Li in the electrolytes of EC/DMC swollen PLPB@PVDF-HFP (a) and PLDB@PVDF-HFP (b).

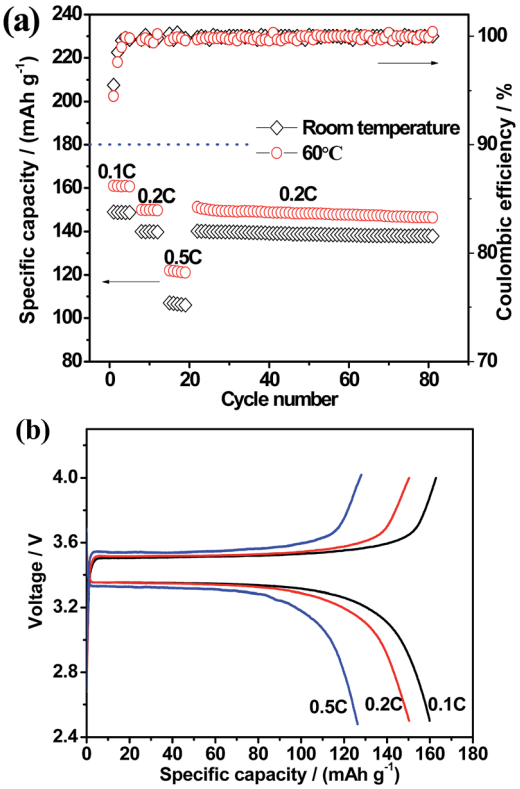

Fig. 7 Rate capability and cycling performance of the Li/EC/DMC swollen PLPB@PVDF-HFP/$LiFePO_4$ batteries at room temperature and 60 °C (a) and charge and discharge profiles of the Li/EC/DMC swollen PLPB@PVDF-HFP/$LiFePO_4$ batteries at 60 °C (b).

demonstrated again that this gel polymer electrolyte was electrochemically and thermally stable, which could fully satisfy the requirement for battery operation.

To further demonstrate the unique performance of the single ion dominantly conducting gel polymer electrolyte, the battery performance at 120 °C was also evaluated where PC was used to replace EC/DMC as the solvent to swell the PLPB@PVDF-HFP membrane owing to its high boiling point. Herein, the battery showed stable cycling performance at 0.5 C for 30 cycles with negligible capacity loss as well as an impressive coulombic efficiency of around 99% (see Fig. S5†), which verified again the electrochemical and thermal stabilities of the GPEs even under such extreme conditions. Considering that the commercial liquid electrolyte could not operate at such high temperatures owing to the thermal instability of $LiPF_6$ and the existence of a large amount of flammable organic solvents, this gel polymer electrolyte containing much less organic solvent could be a very promising alternative for applications in LIBs operating at such high temperatures.

4. Conclusions

In summary, a couple of single-ion polymeric lithium salts were prepared in this study by a facile one-step reaction in aqueous solution. They exhibited uniform morphologies and superior thermal stabilities. The corresponding single ion gel polymer electrolytes EC/DMC swollen PLPB@PVDF-HFP and PLDB@PVDF-HFP exhibited favorable ionic conductivity over a wide temperature range, superior electrochemical stability, significantly high lithium ion transference number and Al passivating ability. The Li/$LiFePO_4$ batteries using these single-ion conducting electrolytes possessed stable charge–discharge behavior and excellent cycle performance both at room temperature and at elevated temperatures. These superior performances could make this class of gel polymer electrolytes very promising candidates for lithium batteries especially at high temperatures.

Acknowledgements

This work was supported by the National Natural Science Foundation of China (Grant no. 21344003), Strategic Priority Research Program of the Chinese Academy of Sciences (Grant no. XDA09010105), Natural Science Foundation of Shandong Province (Grant no. ZR2013FZ2001) and Key Technology Research Projects of Qingdao (Grant no. 12-4-1-24-gx and 13-4-1-10-gx).

Notes and references

1 J. M. Tarascon and M. Armand, *Nature*, 2001, **414**, 359–367.
2 V. Etacheri, R. Marom, R. Elazari, G. Salitra and D. Aurbach, *Energy Environ. Sci.*, 2011, **4**, 3243–3262.
3 M. Armand and J. M. Tarascon, *Nature*, 2008, **451**, 652–657.
4 J. B. Goodenough and K. S. Park, *J. Am. Chem. Soc.*, 2013, **135**, 1167–1176.
5 B. Scrosati, J. Hassoun and Y. K. Sun, *Energy Environ. Sci.*, 2011, **4**, 3287–3295.
6 K. Xu, *Chem. Rev.*, 2004, **104**, 4303–4417.
7 V. Aravindan, J. Gnanaraj, S. Madhavi and H. K. Liu, *Chem.–Eur. J.*, 2011, **17**, 14326–14346.
8 G. G. Botte, R. E. White and Z. Zhang, *J. Power Sources*, 2001, **97–98**, 570–575.
9 C. L. Campion, W. Li and B. L. Lucht, *J. Electrochem. Soc.*, 2005, **152**, A2327–A2334.
10 T. Kawamura, S. Okada and J.-I. Yamaki, *J. Power Sources*, 2006, **156**, 547–554.
11 S. E. Sloop, J. K. Pugh, S. Wang, J. B. Kerr and K. Kinoshita, *Electrochem. Solid-State Lett.*, 2001, **4**, A42–A44.
12 K. Tasaki, K. Kanda, S. Nakamura and M. Ue, *J. Electrochem. Soc.*, 2003, **150**, A1628–A1636.
13 C. Liao, K. S. Han, L. Baggetto, D. A. Hillesheim, R. Custelcean, E. S. Lee, B. K. Guo, Z. H. Bi, D. E. Jiang, G. M. Veith, E. W. Hagaman, G. M. Brown, C. Bridges, M. P. Paranthaman, A. Manthiram, S. Dai and X. G. Sun, *Adv. Energy Mater.*, 2014, **4**, 1301368.
14 R. Rohan, Y. Sun, W. Cai, K. Pareek, Y. Zhang, G. Xu and H. Cheng, *J. Mater. Chem. A*, 2014, **2**, 2960–2967.
15 Z. B. Zhou, M. Takeda, T. Fujii and M. Ue, *J. Electrochem. Soc.*, 2005, **152**, A351–A356.
16 J. Jiang and J. R. Dahn, *Electrochem. Solid-State Lett.*, 2003, **6**, A180–A182.

17 J. Jiang and J. R. Dahn, *Electrochem. Commun.*, 2004, **6**, 724–728.
18 K. Xu, S. Zhang, T. R. Jow, W. Xu and C. A. Angell, *Electrochem. Solid-State Lett.*, 2002, **5**, A26–A29.
19 K. Xu, S. S. Zhang, U. Lee, J. L. Allen and T. R. Jow, *J. Power Sources*, 2005, **146**, 79–85.
20 W. Xu and C. A. Angell, *Electrochem. Solid-State Lett.*, 2001, **4**, E1–E4.
21 S. Shui Zhang, *Electrochem. Commun.*, 2006, **8**, 1423–1428.
22 Q. Wu, W. Lu, M. Miranda, T. K. Honaker-Schroeder, K. Y. Lakhsassi and D. Dees, *Electrochem. Commun.*, 2012, **24**, 78–81.
23 M. Xu, L. Zhou, L. Hao, L. Xing, W. Li and B. L. Lucht, *J. Power Sources*, 2011, **196**, 6794–6801.
24 Y. Zhu, Y. Li, M. Bettge and D. P. Abraham, *J. Electrochem. Soc.*, 2012, **159**, A2109–A2117.
25 S. Zugmann, D. Moosbauer, M. Amereller, C. Schreiner, F. Wudy, R. Schmitz, R. Schmitz, P. Isken, C. Dippel, R. Müller, M. Kunze, A. Lex-Balducci, M. Winter and H. J. Gores, *J. Power Sources*, 2011, **196**, 1417–1424.
26 Y. S. Zhu, X. J. Wang, Y. Y. Hou, X. W. Gao, L. L. Liu, Y. P. Wu and M. Shimizu, *Electrochim. Acta*, 2013, **87**, 113–118.
27 Y. S. Zhu, X. W. Gao, X. J. Wang, Y. Y. Hou, L. L. Liu and Y. P. Wu, *Electrochem. Commun.*, 2012, **22**, 29–32.
28 X. Wang, Z. Liu, Q. Kong, W. Jiang, J. Yao, C. Zhang and G. Cui, *Solid State Ionics*, 2014, **262**, 747–753.
29 X. Wang, Z. Liu, C. Zhang, Q. Kong, J. Yao, P. Han, W. Jiang, H. Xu and G. Cui, *Electrochim. Acta*, 2013, **92**, 132–138.
30 G. Xu, Y. Zhang, R. Rohan, W. Cai and H. Cheng, *Electrochim. Acta*, 2014, **139**, 264–269.
31 Y. Zhang, G. Xu, Y. Sun, B. Han, Teguh Budiono W. T., Z. Chen, R. Rohan and H. Cheng, *RSC Adv.*, 2013, **3**, 14934–14937.
32 Y. Zhu, S. Xiao, Y. Shi, Y. Yang and Y. Wu, *J. Mater. Chem. A*, 2013, **1**, 7790–7797.
33 Y. Zhu, S. Xiao, Y. Shi, Y. Yang, Y. Hou and Y. Wu, *Adv. Energy Mater.*, 2014, **4**, 1300647.
34 B. Qin, Z. Liu, G. Ding, Y. Duan, C. Zhang and G. Cui, *Electrochim. Acta*, 2014, **141**, 167–172.
35 J. Evans, C. A. Vincent and P. G. Bruce, *Polymer*, 1987, **28**, 2324–2328.
36 Z. Cai, Y. Liu, S. Liu, L. Li and Y. Zhang, *Energy Environ. Sci.*, 2012, **5**, 5690–5693.
37 S. Zhang, Z. Chang, K. Xu and C. A. Angell, *Electrochim. Acta*, 2000, **45**, 1229–1236.
38 L. O. Valøen and J. N. Reimers, *J. Electrochem. Soc.*, 2005, **152**, A882–A891.
39 J. Zhao, L. Wang, X. He, C. Wan and C. Jiang, *J. Electrochem. Soc.*, 2008, **155**, A292–A296.
40 W. Xu, A. J. Shusterman, M. Videa, V. Velikov, R. Marzke and C. A. Angell, *J. Electrochem. Soc.*, 2003, **150**, E74–E80.
41 Y. Zhu, F. Wang, L. Liu, S. Xiao, Z. Chang and Y. Wu, *Energy Environ. Sci.*, 2013, **6**, 618–624.